HHS Public Access

Author manuscript

Immunology. Author manuscript; available in PMC 2025 January 01.

Published in final edited form as:

Immunology. 2024 January ; 171(1): 131–145. doi:10.1111/imm.13709.

Structure-guided discovery of aminopeptidase ERAP1 variants capable of processing antigens with novel PC anchor specificities

Suchita Pande[1,2], **Hwai-Chen Guo**[1,*]

[1]Department of Biological Sciences, University of Massachusetts Lowell, 1 University Avenue, Lowell, MA 01854, USA

[2]Present Address: Molecular Cardiology Research Institute, Tufts Medical Center, 800 Washington Street, Boston, MA 02111, USA;

Abstract

Endoplasmic reticulum aminopeptidase 1 (ERAP1) belongs to the oxytocinase subfamily of M1 aminopeptidases (M1APs), which are a diverse family of metalloenzymes involved in a wide range of functions and have been implicated in various chronic and infectious diseases of humans. ERAP1 trims antigenic precursors into correct sizes (8–10 residues long) for MHC (Major Histocompatibility Complex) presentation, by a unique molecular ruler mechanism in which it makes concurrent bindings to substrate N- and C-termini. We have previously determined four crystal structures of ERAP1 C-terminal regulatory domain (termed ERAP1_C domain) in complex with peptide carboxyl (PC)-ends that carry various anchor residues, and identified a specificity subsite for recognizing the PC anchor side chain, denoted as the PC subsite to follow the conventional notations: S1 site for P1, S2 site for P2 etc. Here we report studies on structure-guided mutational and hydrolysis kinetics, and peptide trimming assays to further examine the functional roles of this SC subsite. Most strikingly, a point mutation V737R results in a change of substrate preference from a hydrophobic to a negatively charged PC anchor residue; the latter is presumed to be a poor substrate for WT ERAP1. These studies validate the crystallographic observations that this SC subsite is directly involved in binding and recognition of the substrate PC anchor and presents a potential target to modulate MHC-restricted immunopeptidomes.

Graphical Abstract

*Corresponding author: Hwai-Chen Guo, Department of Biological Sciences, University of Massachusetts Lowell, 1 University Avenue, Lowell, MA 01854, USA, telephone: 978-934-2878, fax: 978-934-3044, HwaiChen_Guo@uml.edu.

Author Contributions

SP and H-CG planned the studies and designed experiments; SP performed experiments and collected data; SP and H-CG analyzed data and wrote the manuscript.

Conflict of interest

The authors declare no conflict of interest.

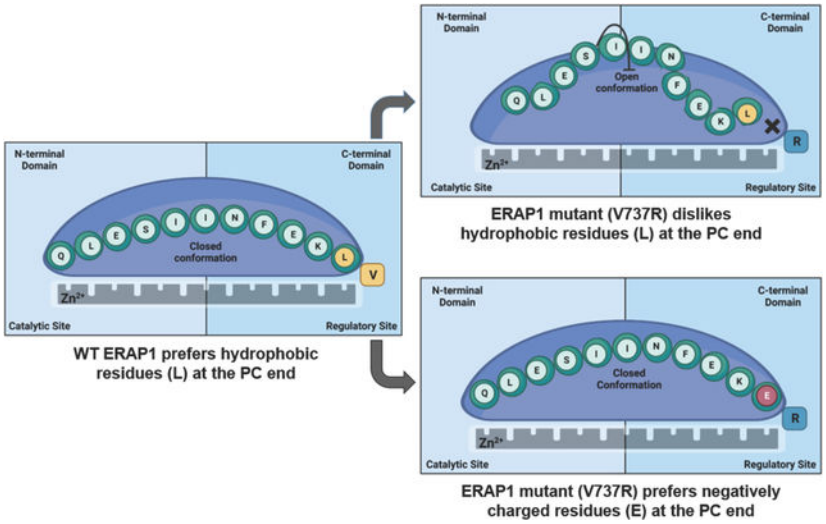

Altering a single amino acid at the SC specificity site of ERAP1, such as the V737R mutant, results in a change of substrate preference from a hydrophobic to a negatively charged PC anchor residue; the latter is presumed to be a poor substrate for WT ERAP1. These results point to a potential target, located ~28 Å away from the canonical S1 site, for selective agents or therapeutics to modulate MHC-restricted immunopeptidomes.

Keywords

specificity SC subsite; peptide carboxyl (PC) anchor; antigen processing kinetics; molecular ruler mechanism; immunopeptidomes

Introduction

Endoplasmic reticulum aminopeptidase 1 (ERAP1) is a member of a diverse family of metalloenzymes called M1 aminopeptidases (M1APs) (1). In humans there are nine characterized and closely related M1APs (2), which are involved in a wide range of functions including cell maintenance, development, and defense, and have been implicated in various chronic and infectious diseases of humans (3–10). The closest clans of ERAP1 are ERAP2 and IRAP (insulin-regulated aminopeptidase) (11–15). These three enzymes belong to the oxytocinase subfamily of M1APs (15) and are integral parts of cell-mediated immune surveillance and responses that involve the major histocompatibility complex (MHC) and subsequent recognition by the appropriate T-cells (9, 16–18). ERAP1 and ERAP2 strongly prefer antigenic peptide precursors of 9–16 residues long but spares peptide of 8–10 residues (19, 20), the latter are the commonly found sizes to fit into the binding cleft of MHC class-I molecules (21, 22). Furthermore, ERAP1 prefers peptides with hydrophobic side chain at the C-termini (23), similar to the binding preference of most MHC-I molecules (24). As such ERAP1 is specialized to process precursors into appropriate MHC-I epitopes. These unusual properties distinguish ERAP1 from a typical aminopeptidase. There are indications that IRAP may also have similar properties (25–27). Thus in shaping the peptide repertoire available for presentation by MHC molecules, these oxytocinases carry out the trimming of

antigen precursors by a unique molecular ruler mechanism in a peptide-length and sequence dependent manner. This activity is enabled by ERAP1's unique capabilities to concurrently bind antigen peptide N- and C-termini by its N-terminal catalytic (peptidase_M1) and C-terminal regulatory (ERAP1_C) domain, respectively (19, 28). Longer precursor peptides with a vast variety of sequences are thought to be sequentially trimmed by the concerted action of ERAP1 and ERAP2 (29, 30). These two enzymes complement and synergize to process antigen precursors with different sequence specificities and anchor residues located at N- and C-termini (31).

Based on four ERAP1_C complex structures and SPR (surface plasmon resonance) binding assays (28, 32, 33), our lab has identified two distinct ERAP1 binding subsites for recognizing the PC (peptide carboxyl)-end of immunopeptidomes: a conserved motif (residues around Tyr684) and a variable specificity SC pocket among oxytocinase subfamily of M1APs (around ERAP1 hydrophobic residues Ile681, Leu733, Leu734, Val737 and Phe803 in Figure 1). They are to recognize the common PC-carboxylate and the variable PC side-chain anchors, respectively. Regardless of differences in PC anchors, internal sequences, and/or lengths, ERAP1 utilizes the same specificity pocket to accommodate and bind different PC anchors: a Leu (32), Phe (33), or His (28). Altogether, these structural analyses and SPR binding assays provide further supports for the proposed molecular ruler mechanism via binding of peptide C-termini by the ERAP1_C regulatory domain. It employs a specificity pocket of ERAP1 to grasp the hydrophobic side chain of the peptide PC anchor. Additional affinity comes from binding of ERAP1 on other common features of peptides such as the backbone and terminal-carboxylate, by making hydrogen-bond contacts using conserved residue Tyr684, and also by forming salt bridges with Lys685 and/or Arg807. Thus the peptide C-terminus recognition by ERAP1_C domain enables the critical trimming of antigen peptides to appropriate lengths in order to fit into the antigen binding cleft of MHC-I molecules (21, 22). Meanwhile ERAP1 also has a somewhat non-discriminatory surface near the middle part of its binding cleft, around a prominent SNP variant at Gln730 (34, 35). These structural features enable ERAP1 to exhibit a high specificity towards peptide N- and C-termini, yet with certain flexibility to accommodate peptides with different internal sequences and lengths (33).

Although it is generally accepted that binding of peptide PC-end by ERAP1 plays a key role in antigen processing, the exact location of the SC subsite for recognizing peptide PC-ends and its functional roles in antigen processing remain controversial (28, 32, 33, 36, 37). To further examine the significance of the putative SC subsite (Figure 1) and its interactions with peptide PC anchor, in this report we have carried out site-directed mutational and kinetics studies of peptide hydrolysis and antigen trimming. We first generated several point mutations that change each hydrophobic residue of the putative SC subsite to a positively charged Arg. We then investigated all purified mutants for their peptide trimming activities using 11-mer peptides designed based on a well-studied ovalbumin-derived MHC Class I-restricted epitope (38). Results indicate that changing these hydrophobic residues to a positively charged Arg has significantly negative impacts on binding and processing activity towards the natural antigen precursor carrying a hydrophobic PC anchor. However, few of them were able to better bind and trim an altered antigen precursor harboring a negatively charged Glu PC anchor, suggesting a critical functional role of the proper SC-PC contacts.

Results

Generation and purification of human ERAP1 mutants using insect cell culture

To evaluate the significance of the hydrophobic SC pocket (Figure 1) in recognizing and processing antigen peptides (immuopeptidomes), we generated single-point mutations at each position of Ile681, Leu733, Leu734, Val737 and Phe803 for catalytic analyses. To this end, each of these five hydrophobic residues were changed to a positively charged arginine, to create five single-point variants designated as I681R, L733R, L734R, V737R and F803R, respectively. ERAP1 WT and mutant enzymes were expressed using an insect-cell system (28, 32, 33), and purified by a protocol with two-step chromatography: an initial capture by IMAC (immobilized metal affinity chromatography) followed by a single-peak elution from a SEC column (size exclusion chromatography). As shown on Figure 2a, with an exception of the I681R mutant, all ERAP1 variants had been purified as a single-major band on an SDS-PAGE gel stained with Coomassie blue.

Monitoring interactions between ERAP1 variants and peptide C-terminus by an allosteric activation assay

Although peptides shorter than 8 residues are not long enough to be efficiently trimmed by ERAP1, they have been shown to be able to activate hydrolysis of small substrate such as the dipeptide analog L-AMC (leucine-7-amido-4-methyl-coumarin) (20, 28). This allosteric effect is postulated to be a result of concurrent bindings of L-AMC and the short peptide to the ERAP1 N-terminal catalytic site and the C-terminal ERAP1_C regulatory site, respectively (32, 33). This unique feature of ERAP1 allows us to analyze interactions between the ERAP1_C and the peptide C-terminus using a three-component assay that contains ERAP1 WT/variant enzyme, small substrate L-AMC for monitoring hydrolysis, and a short peptide to bind to the ERAP1_C domain. For these binding assays we synthesized a pair of 7-mer peptides. One peptide IINFEKL is based on the C-terminal segment of a well-studied ovalbumin-derived MHC Class I-restricted epitope SIINFEKL (19, 38). Binding of the C-terminal end of such a peptide sequence has also been visualized by crystallographic studies (32). For comparative analyses, we also synthesized a second 7-mer IINFEKE which differs from the first peptide by a single a.a. at the PC position, a hydrophobic L (leucine) vs a negatively charged E (glutamic acid). We speculated that with a negatively charged Glu (E) at the PC position, the second IINFEKE peptide may bind better to the mutants that carry a positively charged Arg (R) in the putative SC specificity pocket.

To evaluate the activity of ERAP1 WT and each mutant enzyme, we analyzed L-AMC hydrolysis by the enzymes in the absence or presence of either IINFEKL or IINFEKE peptide (Figures 2b and S1). We first carried out simple activation assays with or without a peptide activator at a fixed concentration (0.1 mM) of L-AMC (Figure S1). Like the ERAP1 WT, each mutant enzyme hydrolyzed L-AMC with a low but detectable basal level in the absence of the peptides (Figure S1, purple columns), suggesting that these mutations at the SC pocket do not prevent substrate binding and catalysis at the catalytic S1 site that is positioned about 28 Á apart (20, 28). It is however noteworthy that the basal activity of mutant I681R, and to a smaller extent L734R, was higher than the other mutant enzymes

and the WT enzyme. One plausible explanation for these different basal activities is that individual mutation has a slightly altered static and/or dynamic conformation, but still retain correct fold to trim peptides (see below). Consistent with this notion, in the SDS-PAGE gel of purified enzymes (Fig 2a), two prominent protein bands below the full length I681R variant were consistently observed in multiple preparations, probably due to a unique conformation of I681R mutant that becomes more susceptible to protease degradation during the purification process. It is also possible that the I681R mutation could have resulted in a conformational changes in the substrate binding groove that allows for better peptide engagement and/or trimming.

In the presence of the peptide containing C-terminal sequence of naturally processed antigenic peptide that had a leucine at the PC position (IINFEKL), a significant increase of ERAP1 aminopeptidase hydrolysis of L-AMC over the basal level was detected for the WT and F803R mutant (Figure S1, blue columns), suggesting an allosteric binding to the regulatory domain. This finding also indicates that the F803R mutation does not alter much of its aminopeptidase activity. The allosteric activation by the IINFEKL peptide was about 75%, 50% and 55% in mutants I681R, L733R and L734R, respectively, when compared to that of the wildtype enzyme. Mutant V737R had the lowest activity in the presence of IINFEKL peptide and with the smallest activation from its basal activity.

In the presence of the second peptide (IINFEKE) carrying a negatively charged PC residue that is considered to be a poor substrate for WT ERAP1 (23), the aminopeptidase activities of ERAP1 WT and most mutants were not activated significantly above their basal levels (Figure S1, orange columns). The only exception in this assay is mutant V737R that gains a slight but significant activation (~ 30%) from its basal activity in the presence of IINEKE peptide. Interesting to note that this single-point mutation at residue 737, from a hydrophobic valine to a positively charged arginine, appears to make the enzyme more accommodating to a negatively charged glutamic acid at the substrate PC-terminus, suggesting that this Val737 is involved in binding to the PC-terminus of antigenic peptides.

Hydrolysis kinetics of dipeptide analog L-AMC using short peptide as an effector

We further compared the hydrolysis of ERAP1 and variants by steady state kinetics in the presence or absence of a peptide activator (Figure 2b). To this kinetic assay, we follow hydrolysis of L-AMC at varying concentrations (0.001–2 mM). In the absence of peptide activator, mutations L733R and V737R have the largest negative impacts on the initial rate and Vmax (blue curves in Figure 2b, and Table 1), most apparent at high concentrations of substrate (e.g. at 2 mM on the right side of graphs in Figure 2b). Nonetheless all variants showed a similar initial rate vs. substrate concentration curve that did not follow simple Michaelis-Menten kinetics, but exhibited an allosteric sigmoidal velocity curve (blue curves in Figure 2b). Consistent with previous reports (20), these sigmoid curves are characteristic of positive cooperativity of enzymes with one or more ligand binding sites. Our gel filtration results suggest that ERAP1 WT and mutant enzymes were purified predominantly in a monomeric form (data not shown). It is however possible that the regulatory site can be occupied by L-AMC as a homotropic allosteric activator, leading to the positive cooperativity and allosteric sigmoidal activation of the enzymes in the absence of peptides.

The Hill coefficients (h, measure of cooperative binding) for ERAP1 WT without peptides was calculated to be 2.6 (Table 1) and is comparable to the previously reported value (20). F803R had a same h value as the WT. For mutants I681R, L733R, L734R, V737R, the h values were 1.8, 1.5, 1.3 and 1.9, respectively. The lower Hill coefficients of these mutants suggest that the hydrophobic pocket targeted by this mutational study is involved in this homotropic allosteric activation.

Strikingly, in the presence of IINFEKL peptide, the velocity curves of all variants followed more like a hyperbolic (Michaelis-Menten) kinetics with reduced cooperativity (smaller h values), except L734R that had a slightly increased h (Table 1). Meanwhile ERAP1 WT and variants all have a significant or dramatic increase of Vmax, mostly apparent the WT and F803R mutant (green curves in Fig 2b). These results indicate that the allosteric activity of the enzymes was “switched further on” after the addition of peptide IINFEKL. Several classical enzyme systems have long been reported in which addition of an allosteric activator/effector molecule increases the affinity of enzyme for the substrate and shifts the sigmoidal curve to a more hyperbolic curve with increased reaction velocity (39–41). On the other hand, addition of IINFEKE peptide did not change much the sigmoidal curves (magenta curves in Fig 2b), h values, or Vmax for most enzyme variants (Table 1), suggesting weak binding of this peptide to the hydrophobic or mutated pocket. Nonetheless, consistent with data in Figure S1, mutant V737R appeared to be significantly activated by the peptide IINFEKE (see the zoom-in inset in Figure 2b), with a concurrently reduction of h value and an increase of Vmax (Table 1), indicating that the IINFEKE peptide is able to switch the V737R mutant “further on” to a more hyperbolic kinetics”, similar to IINFEKL did to the WT enzyme. These small but significant activations of V737R by the peptide IINFEKE over IINFEKL or the basal level (L-AMC alone) were confirmed by Brown-Forsyth one-way ANOVA and Tukey’s multiple comparisons test (Fig 2c).

Furthermore, by comparing $K_{1/2}$ values (half Vmax concentration of L-AMC) of WT or F803 mutant (Table 1), IINFEKL afforded a low (~0.19 mM) $K_{1/2}$ value when compared to IINFEKE or L-AMC itself (0.34–0.38 mM), indicating IINFEKL was an effective allosteric activator on WT and F803 mutant. However, IINFEKL did not exert the same effect on $K_{1/2}$ of other variants, suggesting an impairment of the allosteric interactions between the mutated hydrophobic pocket of ERAP1 and the IINFEKL activator (Table 1). For V737R mutant, although IINFEKE was able to somewhat offset the mutation by an allosteric activation, it is not a very effective activator with a relatively high $K_{1/2}$ (0.45 mM, see Table 1).

To further investigate the effect of mutations on binding affinity of peptide activators, we analyzed the hydrolysis kinetics of L-AMC at a fixed concentration (0.1 mM) but with varying concentrations (0.001–2 mM) of peptide effector IINFEKL (Figure 3). With the exception of I681 R, all other variants show a similar hyperbolic curve but at different levels. WT ERAP1 had the largest Vmax and the smallest AC50 value (half maximal activation concentration of IINFEKL), whereas the V737R mutant had the smallest Vmax and one of the largest AC50 value (Figure 3 and Table 2). Other variants fell in between in the order of F803R, L733R, and L734R, with a decreasing value in Vmax and a concurrent increase of value in AC50, indicating these mutants could still bind to the IINFEKL but with a lower

affinity for activation. The activation curve of I681R appeared to be unique, with a shallower slope throughout the entire range of IINFEKL concentrations examined, resulting in a much higher AC50 estimate of 1.46 mM. This deviation could be results of protease degradation (Figure 2a) and/or a higher intrinsic/basal activity due to a subtle conformational change (Figure S1).

N terminal trimming of antigenic peptides by ERAP1 WT and mutant enzymes

We also evaluated and compared peptide trimming activities of ERAP1 WT and variants using a well-studied antigen precursor QLESIINFEKL, which has the same C-terminal sequence as the 7-mer effector used in the activation assays above (Figures. 2–3). This 11-mer antigenic substrate contains the ovalbumin-derived MHC Class I-restricted epitope SIINFEKL, and has been shown to be efficiently processed by ERAP1 (19, 20, 38). A companion 11-mer peptide QLESIINFEKE was also used for comparative studies by LC-MS analyses. These two peptide substrates only differ by one residue at the peptide PC position, a hydrophobic leucine (L) vs a negatively charged glutamic acid (E). This pair of 11-mer peptides were designed to examine how the presence of a positively charged arginine residue in the hydrophobic pocket of ERAP1 mutants would affect recognition and processing of peptide substrates that have either a hydrophobic or a complementing negatively charged PC anchor

To follow peptide-trimming efficiency of each enzyme variant, we used liquid chromatography mass spectrometry (LC-MS/MS) to monitor a decrease of the 11-mer substrate QLESIINFEKL (KL1), and concurrent generation and further cleavage of the first (10-mer) product LESIINFEKL (KL2). As shown in Figure 4, ERAP1 WT and mutant F803R were able to efficiently process 11-mer QLESIINFEKL (KL1) at its N-terminal to generate the 10-mer product LESIINFEKL (KL2). After 10-min, the amount of this 10-mer KL2 product began to decrease, indicating ERAP1 WT and mutant F803R were able to further process it (Figure 4b). Consistent with this trimming trend, there was concurrent increase and subsequent decrease of the second (9-mer) intermediate ESIINFEKL (KL3) peptide (Figure S2). However, the other mutants processed these peptides at a slower rate (Figures 4 and S2). Mutant V737R was the slowest to process this series of peptides. These results are consistent with the L-AMC hydrolysis assays above using IINFEKL peptide as an activator (Figures 2–3).

We also analyzed trimming efficiency of the second peptide by each enzyme variant, from the 11-mer substrate QLESIINFEKE (KE1) to the first (10-mer) product/intermediate LESIINFEKE (KE2) (Figure 5). Interestingly, the rate of processing from KE1 to KE2 by V737R mutant was the fastest, followed by L734R and I681R mutants, while the peptide trimmings by WT, F803R and L733R were slower (Fig 5 a–b). Again, these results agree with the L-AMC hydrolysis activation assay above, where the allosteric activation of ERAP1 WT, L733R and F803R enzymes by IINFEKE peptide did not show significant difference from their respective basal activity (Figures 2 and S1). Together these results suggest that binding of IINFEKE sequence to ERAP1 WT, L733R and F803R is poor and hence, peptide substrates containing C-terminal IINFEKE sequence are processed at a much slower rate. On the other hand I681R and L734R appears to process KE1 and KE2 peptides with a

higher rate. However, as pointed out earlier, the latter two variants also have a higher basal L-AMC hydrolysis in the absence of any activator (Figure S1), suggesting that these two mutations could have generated substantial conformational changes that result in an elevated aminopeptidase activity without interacting with substrate PC-end. Among ERAP1 WT and variants, the V737R mutant was the most efficient enzyme to process substrates KE1 and KE2 (Figure 5). This is consistent with results above from activation assays that demonstrate IINFEKE was able to activate L-AMC hydrolysis of V737R mutant significantly (~30%) above its basal activity, either in the simple activation assays (Figure S1) or by steady state kinetics studies (Figure 2b–c).

We also compared and analyzed each mutant the depletion of 11-mer precursor peptide (KL1 vs KE1 in Figure 6) and accumulation followed by trimming of the 10-mer intermediate (KL2 vs KE2 in Figure 7). It is evident that ERAP1 WT as well as F803R were able to process KL1 and KL2 peptides far more efficiently than KE1 and KE2, followed by L733R. The processing patterns are reversed for I681R, L734R, and V737R mutants. For peptides with a Glu PC anchor, WT and F803R were less efficient to process KE1 (Figures 6a & 6f), concurrently with a slower accumulation of KE2 as well a slower disappearance of KE2 via subsequent cleavage (Figures 7a & 7f). In contrast, these substrate profiles were reversed for the V734R and V737R mutants: they are more efficient to process KE1 (Figures 6d & 6e), concurrently with and a faster accumulation of KE2 as well a faster disappearance of KE2 via subsequent cleavage (Figures 7d & 7e). Among all variants, V737R was the most efficient in processing KE1 and KE2 peptides that carry a complementary charged anchor residue (E) at their PC position.

Discussion

ERAP1 trims antigenic precursors in a sequence and length dependent manner, to generate final antigens with an appropriate size for MHC presentation (19). It thus acts as a molecular ruler by binding simultaneously to the peptide N- and C-termini, using its N-terminal peptidase_M1 and C-terminal ERAP1_C domain, respectively. Several crystal structures of ERAP1 in complex with different peptide sequences and lengths have been reported (28, 32, 33, 37). Based on these structural analyses we had identified two distinct subsites in ERAP1_C to recognize the peptide PC termini: a conserved motif (Tyr684 and Arg841) and a variable specificity pocket among oxytocinase subfamily of M1APs (the SC subsite around ERAP1 Val737 in Figure 1) to bind to the common peptide backbone/carboxylate and the variable anchor residue at the PC position, respectively. To correlate structure-function relationships and investigate functional roles of these SC-PC interactions, in this report we have generated several structure-guided point mutations that change each of these hydrophobic side chains to a positively charged Arg: I681R, L733R, L734R, V737R, and F803R. All mutant proteins have been purified and analyzed for their peptidase activity by studying dipeptide analog L-AMC hydrolysis and kinetics, and long peptide trimming. Results showed that ERAP1 WT is able to process peptides with a Leu PC anchor far more efficiency than peptides with a Glu PC anchor. In contrast, the processing patterns of a few mutants, particularly V737R, are reversed, such that they are more efficient in processing peptides with a Glu PC anchor than the natural antigenic epitope carrying a Leu PC anchor. Furthermore, we also investigated kinetics of dipeptide analog L-AMC

hydrolysis with or without a 7-mer peptide that carries either a Leu or Glu PC anchor. Altogether, these findings validate the crystallographic observations that Ile681, Leu733, Leu734 and Val737 are directly involved in binding and recognizing substrate peptide PC anchor for the allosteric activation of aminopeptidase activity through the molecular ruler mechanism. As such a point mutation like V737R would result in an enzyme that prefers a substrate carrying a complementary PC anchor, e.g. the KE1 peptide precursor. Interestingly, Val737 was identified as an SNP polymorphism associated with ankylosing spondylitis (42), likely due to a result of altering MHC-I restricted immunopeptidomes. However, in a large-scale analysis of common ERAP1 allotypes, none of the SC positions studied in this report has been concluded as a top-ten polymorphic residue (43). An interesting question awaiting to be addressed is whether these newly generated ERAP1 variants could trim peptide precursors down to 8-mer SIINFEKL or SIINFEKE epitopes.

ERAP1 structure consists of 4 subdomains I-IV, with a more conserved N-terminal peptidase_M1 domain (subdomains I+II) and a more variable ERAP1_C domain (subdomains III+IV). Two different conformations of ERAP1 have been found inside crystals: an open and a closed conformation (20, 44). It had been postulated that in the molecular ruler mechanism a concurrent binding of the peptide N- and C-termini in ERAP1 would switch the enzyme from the low-activity open conformation to a high-activity closed conformation (28, 32, 45), by bringing subdomains II and IV together. Interestingly, the I681R mutant studied in this report appears to be more susceptible to protease degradation (extra bands in Figure 2a), probably as a result of acquiring a new conformation, and was also switched to a high basal-activity mode without peptide activation (Figure S1). Further analyses are needed regarding the nature of these extra protein bands, and their effects on enzymatic measurements. In addition to be part of the SC specificity pocket, Ile681 is also located in an α-helix (residues Glu669-Lys689Lys) that was hinged closer (via subdomain III) to another α-helix of subdomain II (residues Tyr399-Ala412) to make additional contacts, resulting in the closed conformation (e.g. Asp406 in contact with Asn678). Hence, similar to other interdomain interactions described elsewhere (46), the I681R mutation may have altered the molecular dynamics and/or energetic barrier for the allosteric transition from the open to the closed conformations.

MHC class-I molecules are known to prefer different PC anchor residues, but predominantly with either a hydrophobic or a positively charged side chain (21, 24, 47). In concert, ERAP1 also has dual specificities on the substrate PC anchor, either a hydrophobic or a positively charged side chain (23) to generate appropriate immunopeptidomes for MHC presentation. While this study targets at the SC specificity pocket for binding a hydrophobic anchor, peptides with a charged PC anchor would need to be accommodated into a different specificity pocket. In a crystal structure of ERAP1-peptide complex, a 10-mer peptide analog was found to place its positively charged Lys PC anchor near Asp766 of ERAP1 through a salt bridge interaction (37). However, validity of this charged SC site to bind a positively charged PC anchor remains to be confirmed since the interaction between PC Lys and ERAP1 residues in the crystals appears to be limited. Another potential charged specificity pocket with more extensive interactions to bind peptides with a positively charged Lys or Arg PC anchor had been proposed previously: around Glu802 and Glu831 of ERAP1 (28). For binding by this latter putative charged SC subsite, the conserved Arg841 of ERAP1

can make direct contacts with the peptide PC-carboxylate to provide additional binding affinity.

Although peptides shorter than 8 residues are not long enough to be efficiently trimmed by ERAP1 at the S1 site, they have long been demonstrated to be able to allosterically activate in *trans* the hydrolysis of a second substrate bound at the S1 site, likely by binding the short peptide to the SC site of ERAP1_C domain (20, 28, 32, 33). Using the L-AMC + IINFEKL trimming assays, we were able to report here $K_{1/2}$ of L-AMC and AC_{50} of IINFEKL for S1 and SC binding affinities, respectively (Tables 1 and 2). Recently, small molecules have also been discovered by crystallography or computationally docking to bind to the conserved PC binding motif, and are found to affect in *trans* ERAP1 activity in a way similar to a short peptide (48–50). However as pointed out above, that conserved PC binding motif (around Tyr684) is different from the hydrophobic SC pocket studied here (Ile681, Leu733, Leu734, Val737 and Phe803 in Fig. 1). This novel and variable SC pocket studied in this report presents an exciting target, located ~28 Å away from the canonical S1 site (28), for structure-guided screen and design of selective agents or therapeutics to modulate ERAP1 functions in antigen processing and presentation (2, 16, 51, 52). It may also present an opportunity to engineer a novel oxytocinase that could alter the immunopeptidomes by processing and generating antigenic peptides harboring a “poor or impermissible” anchor at the PC position (such as carrying a PC Glu like the KE1 peptide studied in Figure 6).

Materials and Methods

Site-directed mutagenesis

Mutagenesis to introduce the five point mutations into ERAP1 (I681R, L733R, L734R, V737R and F803R) were carried out by a three-stage PCR amplification, using a template plasmid reported previously (28), carrying ERAP1 gene of the common allotype-1 (15, 43). Briefly two site-directed mutated fragments were generated first using mutant-specific forward/reverse primers and the attL1/L2 universal primers, with ~25–27 bp overlap between the two mutant-specific primers that cover the mutated site. In the next step, PCR products of two overlapped mutant-specific fragments (generated from step 1) were mixed in a ratio of 1:1 without any primers and PCR-amplified for 5 cycles. Due to the overlap in the mutant-specific fragments, a hybrid DNA containing the mutation was generated with a poly-His tag sequence at the 3’ end (for protein purification) flanked by the attL1 and attL2 universal primer sequence. In step 3, the entire mutant genes were further PCR-amplified for 30 cycles using attL1 and attL2 universal primers. The sequences of mutant-specific primers were (5′−3′) as follows: I681R_F, GTTTGAATGAGCTGAGGCCTATGTATAAGTTAATGGAGAAAAGAGATATGAATGAAGTG; I681R_R, TAACTTATACATAGGCCTCAGCTCATTCAAACCTTGAAACACGGG; L733R_F, GTCAACTACTACGCCTCGCCTGTGTGCACAACTATCAGCCG; L733R_R, ACACAGGCGAGGCGTAGTAGTTGACTCCGCAGCATTCGCTC; L734R_F, CAACTACTACTCCGCGCCTGTGTGCACAACTATCAGCCG; L734R_R, GTGCACACAGGCGCGGAGTAGTAGTTGACTCCGCAGCATTCG; V737R_F, CTCCTCGCCTGTCGGCACAACTATCAGCCGTGCGTACAGAGGG; V737R_R, CTGATAGTTGTGCCGACAGGCGAGGAGTAGTAGTTGACTCCGC; F803R_F,

AGCCAAATTGAACGTGCCCTCTGCAGAACCCAAAATAAGGAAA; F803R_R, TCTGCAGAGGGCACGTTCAATTTGGCTTTTCTCAGTACTGGAC.

Recombinant ERAP1 expression and purification

Expression clone of each mutant was generated according to the manufacturer's instructions (Invitrogen). Sequences of all selected mutants were verified by DNA sequencing. Expression clone of the wild-type (WT) or mutant was transformed into DH10Bac competent cells. White colonies were then selected for isolation of recombinant bacmid. To confirm the correct insertion of the gene of interest in the bacmid DNA, PCR was performed using M13 forward and reverse primers followed by electrophoresis of PCR products on 1% DNA agarose gel. The bacmid DNA was then transfected to insect Sf9 cells growing in SF-900 II serum-free medium (Thermo Fisher Scientific), according to the manufacturer's instructions. When the signs for transfection appeared, the culture medium containing recombinant baculovirus (V0) was collected by centrifugation for 6 minutes at 700g. Two amplification rounds were carried out to generate recombinant baculoviral stock with higher titer (V1 and V2). The V2 titers of WT and mutant viral stocks were determined by viral plaque assay to be 1–2 × 108 PFU/ml. To determine the optimal MOI and time of post-infection for best protein expression yield, culture samples with varying MOI (0.5, 1, 2 and 4 pfu/cell) and at various post-infection incubation (48, 72 and 96 hours) were collected and analyzed by Western blotting.

WT and mutant ERAP1 enzymes were expressed in *Spodoptera frugiperda* (Sf9) insect cells via Bac-to-Bac baculoviral expression system by a method modified from previously described approaches (53, 54). Each of these enzyme variants with a C-terminal His_6-tag was purified from a 400-ml cell culture using Ni-NTA affinity chromatography. Briefly, Sf9 insect cell culture was pelleted by centrifuging at 700g using Sorvall Dupont HS-4 rotor for 10 min. The cell pellet was re-suspended in binding buffer (50mM Tris HCl, pH 7.5, 300mM NaCl and 10mM imidazole) and lysed by 3 cycles of sonication for 10 seconds on ice with 20 seconds break in-between. Soluble protein in the supernatant was separated from cell debris by high-speed centrifugation using a SS-34 rotor at 13,000g for 55 minutes at 4°C. The supernatant was loaded onto a pre-equilibrated Ni-NTA resin in a gravity flow column (Bio-Rad), which was further washed 5x with a wash buffer (50mM Tris HCl, pH 7.5, 300mM NaCl and 30mM imidazole). The histidine-tagged recombinant protein was then eluted with elution buffer (50mM Tris HCl, pH 7.5, 300mM NaCl and 400mM imidazole). The entire purification process was performed at 4°C.

The eluted proteins from Ni-NTA resin were concentrated to ~4 mg/ml in 500μl for further purification with a Superdex 200 Increase gel filtration column (Cytiva). Before loading to the column, 16% (v/v) glycerol was added to the concentrated protein sample to stabilize it. Separation was carried out with running buffer containing 10mM Tris HCl, pH 7.5 and 10mM NaCl. The first peak was aggregation peak, the second peak was the ERAP1 full length peak, and the third peak was the degraded ERAP1 C-terminal. The second peak of protein, eluted around 12 ml, was collected and concentrated to 0.5 to 1 mg/ml.

To quantify ERAP1 wildtype and mutant proteins, different concentrations (1, 0.5, 0.25 and 0.125 mg/ml) of bovine serum albumin (BSA) protein (Thermo Fisher Scientific) were

prepared in the gel filtration buffer as standards. Equal volume (8ul) of BSA standards and ERAP1 (wildtype and mutants) proteins were then loaded onto an SDS-PAGE gel for quality and quantity analysis. The protein concentration of the ERAP1 proteins was estimated by comparing it to the protein standard bands on the gel. From each 400-ml culture, approximately 0.05 to 0.25 mg of protein was obtained for ERAP1 WT or variants.

Enzyme Activation Assays

Aminopeptidase activity for ERAP1 WT and mutant enzymes was determined by measuring fluorescence of 7-amido-4-methylcoumarin (AMC) release from hydrolysis of the dipeptide analog Leucine-AMC (L-AMC) (Figure S1). The assays were performed in 200 μl buffer composed of 50 mM Tris/HCl (pH 8.0), 0.1 M NaCl, containing 1.5 μg ml^{-1} of enzyme in the presence or absence of 100 μM IINFEKL or IINFEKE peptide (Genescript) at 25°C. Hydrolysis of 100 μM L-AMC was followed for 5 minutes and hydrolyzed AMC was measured using an excitation wavelength of 380 nm and an emission wavelength of 460 nm. Fluorescence intensities were calibrated using AMC as standards.

Kinetics Studies of Peptidase Activation by 7-mer Peptides

Kinetic studies of L-AMC hydrolysis activated by 7-mer peptides were performed to determine kinetic parameters. Each reaction contained 1.5 μg ml^{-1} ERAP1 (WT or mutants) with varying concentrations (0–2,000 μM) of L-AMC (in Figure 2b) or peptide (IINFEKL in Figure 3) in a buffer containing 50 mM Tris/HCl (pH 8.0), 0.1 M NaCl at 27 °C, and with either 100 μM of peptide if applicable (in Figure 2b) or L-AMC (in Figure 3). Hydrolysis of L-AMC was followed for 5 minutes and hydrolyzed AMC was measured using an excitation wavelength of 380 nm and an emission wavelength of 460 nm. Curve fitting to obtain Vmax, half-Vmax concentration $K_{1/2}$ of L-AMC, half maximal activation concentration AC_{50} of peptide activator, and the cooperativity Hill coefficient (h) values were calculated using the Prism 8 software, GraphPad (https://www.graphpad.com/scientific-software/prism/). Statistics were performed by Brown-Forsyth one-way ANOVA and Tukey's multiple comparisons test, using GraphPad Prism 8 software.

Peptide Trimming Assays

100 nmoles of the 11-mer peptide QLESIINFEKL or QLESIINFEKE (synthesized by Genescript, Piscataway, NJ) were incubated at 30 °C with 3.5 μg of ERAP1 WT or mutant enzyme in 1ml of 50 mM Tris pH 7.8 containing 0.5 μg protease free bovine serum albumin (Sigma Aldrich, Louis, MO) in a time course experiment (aliquoted at 0.5, 1, 2, 5, 10, 30, 60, 90, & 120 minutes). The reaction was stopped by adding formic acid to a final concentration of 1% (v/v). Samples were then run through a Shim-pack GWS C18 column (150 mmL. × 4.6 mmI.D., 5μm, Shimadzu) and analyzed by LC-MS/MS (Shimadzu lcms 8040). Peptide separation was performed using an 8 min gradient running from 5% acetonitrile, 0.1% formic acid in H2O to 100% acetonitrile, 0.1% formic acid in H2O at a flow rate of 0.5 ml/min. Quantitative data was obtained by the generation and integration of multiple reaction monitoring (MRM) of the product ions of each peptide intermediate using the Lab Solutions Analysis Software (Shimadzu). For normalization, the areas of all MRMs observed in each time point were added together, and the signal of each peptide intermediate was calculated as a percentage of the sum of all MRMs. 100, 50, 25, 12.5,

6.25 nmol standards of peptides were used to quantify trimming and generation of peptide fragments.

Supplementary Material

Refer to Web version on PubMed Central for supplementary material.

Acknowledgements

We thank William Bizilj for assistance on kinetic studies, and Adam Luk on manuscript preparation. This work was supported by Grant GM128152 from the NIH.

Abbreviations:

ER	endoplasmic reticulum
ERAP1	endoplasmic reticulum aminopeptidase 1
ERAP1_C	ERAP1 C-terminal regulatory domain
MHC	major histocompatibility complex
PC	peptide carboxyl-terminus
SC subsite	specificity site of ERAP1 to bind peptide substrate at the PC anchor side chain

Enzyme:

endoplasmic reticulum aminopeptidase 1 (ERAP1)
EC # 3.4.11.1

References

1. Rawlings ND, Bateman A. How to use the MEROPS database and website to help understand peptidase specificity. Protein Sci. 2021;30(1):83–92. [PubMed: 32920969]
2. Drinkwater N, Lee J, Yang W, Malcolm TR, McGowan S. M1 aminopeptidases as drug targets: broad applications or therapeutic niche? FEBS J. 2017;284(10):1473–88. [PubMed: 28075056]
3. Peer WA. The role of multifunctional M1 metallopeptidases in cell cycle progression. Ann Bot. 2011;107(7):1171–81. [PubMed: 21258033]
4. Cifaldi L, Romania P, Lorenzi S, Locatelli F, Fruci D. Role of endoplasmic reticulum aminopeptidases in health and disease: from infection to cancer. Int J Mol Sci. 2012;13(7):8338–52. [PubMed: 22942706]
5. Alvarez-Navarro C, Lopez de Castro JA. ERAP1 in ankylosing spondylitis: genetics, biology and pathogenetic role. Curr Opin Rheumatol. 2013;25(4):419–25. [PubMed: 23656713]
6. Alvarez-Navarro C, Lopez de Castro JA. ERAP1 structure, function and pathogenetic role in ankylosing spondylitis and other MHC-associated diseases. Mol Immunol. 2014;57(1):12–21. [PubMed: 23916068]
7. Leone P, Shin EC, Perosa F, Vacca A, Dammacco F, Racanelli V. MHC class I antigen processing and presenting machinery: organization, function, and defects in tumor cells. J Natl Cancer Inst. 2013;105(16):1172–87. [PubMed: 23852952]

8. Agrawal N, Brown MA. Genetic associations and functional characterization of M1 aminopeptidases and immune-mediated diseases. Genes Immun. 2014;15(8):521–7. [PubMed: 25142031]

9. Fruci D, Romania P, D'Alicandro V, Locatelli F. Endoplasmic reticulum aminopeptidase 1 function and its pathogenic role in regulating innate and adaptive immunity in cancer and major histocompatibility complex class I-associated autoimmune diseases. Tissue Antigens. 2014;84(2):177–86. [PubMed: 25066018]

10. Lopez de Castro JA, Alvarez-Navarro C, Brito A, Guasp P, Martin-Esteban A, Sanz-Bravo A. Molecular and pathogenic effects of endoplasmic reticulum aminopeptidases ERAP1 and ERAP2 in MHC-I-associated inflammatory disorders: Towards a unifying view. Mol Immunol. 2016;77:193–204. [PubMed: 27522479]

11. Serwold T, Gonzalez F, Kim J, Jacob R, Shastri N. ERAAP customizes peptides for MHC class I molecules in the endoplasmic reticulum. Nature. 2002;419(6906):480–3. [PubMed: 12368856]

12. Saric T, Chang SC, Hattori A, York IA, Markant S, Rock KL, et al. An IFN-gamma-induced aminopeptidase in the ER, ERAP1, trims precursors to MHC class I-presented peptides. Nat Immunol. 2002;3(12):1169–76. [PubMed: 12436109]

13. Tanioka T, Hattori A, Masuda S, Nomura Y, Nakayama H, Mizutani S, et al. Human leukocyte-derived arginine aminopeptidase. The third member of the oxytocinase subfamily of aminopeptidases. J Biol Chem. 2003;278(34):32275–83. [PubMed: 12799365]

14. Saveanu L, Carroll O, Hassainya Y, van Endert P. Complexity, contradictions, and conundrums: studying post-proteasomal proteolysis in HLA class I antigen presentation. Immunol Rev. 2005;207:42–59. [PubMed: 16181326]

15. Tsujimoto M, Hattori A. The oxytocinase subfamily of M1 aminopeptidases. Biochim Biophys Acta. 2005;1751(1):9–18. [PubMed: 16054015]

16. Hanson AL, Morton CJ, Parker MW, Bessette D, Kenna TJ. The genetics, structure and function of the M1 aminopeptidase oxytocinase subfamily and their therapeutic potential in immune-mediated disease. Human immunology. 2019;80(5):281–9. [PubMed: 30419264]

17. Babaie F, Hosseinzadeh R, Ebrazeh M, Seyfizadeh N, Aslani S, Salimi S, et al. The roles of ERAP1 and ERAP2 in autoimmunity and cancer immunity: New insights and perspective. Mol Immunol. 2020;121:7–19. [PubMed: 32135401]

18. Yang X, Garner LI, Zvyagin IV, Paley MA, Komech EA, Jude KM, et al. Autoimmunity-associated T cell receptors recognize HLA-B*27-bound peptides. Nature. 2022.

19. Chang SC, Momburg F, Bhutani N, Goldberg AL. The ER aminopeptidase, ERAP1, trims precursors to lengths of MHC class I peptides by a "molecular ruler" mechanism. Proc Natl Acad Sci U S A. 2005;102(47):17107–12. [PubMed: 16286653]

20. Nguyen TT, Chang SC, Evnouchidou I, York IA, Zikos C, Rock KL, et al. Structural basis for antigenic peptide precursor processing by the endoplasmic reticulum aminopeptidase ERAP1. Nat Struct Mol Biol. 2011;18(5):604–13. [PubMed: 21478864]

21. Guo H-C, Jardetzky TS, Garrett TPJ, Lane WS, Strominger JL, Wiley DC. Different length peptides bind to HLA-Aw68 similarly at their ends but bulge out in the middle. Nature. 1992;360(6402):364–6. [PubMed: 1448153]

22. Silver ML, Guo H-C, Strominger JL, Wiley DC. Atomic structure of a human MHC molecule presenting an influenza virus peptide. Nature. 1992;360(6402):367–9. [PubMed: 1448154]

23. Evnouchidou I, Momburg F, Papakyriakou A, Chroni A, Leondiadis L, Chang SC, et al. The internal sequence of the peptide-substrate determines its N-terminus trimming by ERAP1. PLoS ONE. 2008;3(11):e3658. [PubMed: 18987748]

24. Rammensee H, Bachmann J, Emmerich NP, Bachor OA, Stevanovic S. SYFPEITHI: database for MHC ligands and peptide motifs. Immunogenetics. 1999;50(3–4):213–9. [PubMed: 10602881]

25. Ascher DB, Cromer BA, Morton CJ, Volitakis I, Cherny RA, Albiston AL, et al. Regulation of insulin-regulated membrane aminopeptidase activity by its C-terminal domain. Biochemistry. 2011;50(13):2611–22. [PubMed: 21348480]

26. Hermans SJ, Ascher DB, Hancock NC, Holien JK, Michell BJ, Chai SY, et al. Crystal structure of human insulin-regulated aminopeptidase with specificity for cyclic peptides. Protein Sci. 2015;24(2):190–9. [PubMed: 25408552]

27. Mpakali A, Saridakis E, Giastas P, Maben Z, Stern LJ, Larhed M, et al. Structural Basis of Inhibition of Insulin-Regulated Aminopeptidase by a Macrocyclic Peptidic Inhibitor. ACS Med Chem Lett. 2020;11(7):1429–34. [PubMed: 32676150]
28. Gandhi A, Lakshminarasimhan D, Sun Y, Guo H-C. Structural insights into the molecular ruler mechanism of the endoplasmic reticulum aminopeptidase ERAP1. Sci Rep. 2011;1:186. [PubMed: 22355701]
29. Saveanu L, Carroll O, Lindo V, Del Val M, Lopez D, Lepelletier Y, et al. Concerted peptide trimming by human ERAP1 and ERAP2 aminopeptidase complexes in the endoplasmic reticulum. Nat Immunol. 2005;6(7):689–97. [PubMed: 15908954]
30. Lorente E, Barriga A, Johnstone C, Mir C, Jimenez M, Lopez D. Concerted in vitro trimming of viral HLA-B27-restricted ligands by human ERAP1 and ERAP2 aminopeptidases. PLoS One. 2013;8(11):e79596. [PubMed: 24223975]
31. Martín-Esteban A, Rodriguez JC, Peske D, Lopez de Castro JA, Shastri N, Sadegh-Nasseri S. The ER Aminopeptidases, ERAP1 and ERAP2, synergize to self-modulate their respective activities. Front Immunol. 2022;13:1066483. [PubMed: 36569828]
32. Sui L, Gandhi A, Guo H-C. Crystal structure of a polypeptide's C-terminus in complex with the regulatory domain of ER aminopeptidase 1. Mol Immunol. 2016;80:41–9. [PubMed: 27825049]
33. Sui L, Guo H-C. ERAP1 binds peptide C-termini of different sequences and/or lengths by a common recognition mechanism. Immunobiology. 2021;226(4):152112. [PubMed: 34247019]
34. Harvey D, Pointon JJ, Evans DM, Karaderi T, Farrar C, Appleton LH, et al. Investigating the genetic association between ERAP1 and ankylosing spondylitis. Hum Mol Genet. 2009;18(21):4204–12. [PubMed: 19692350]
35. Stamogiannos A, Koumantou D, Papakyriakou A, Stratikos E. Effects of polymorphic variation on the mechanism of Endoplasmic Reticulum Aminopeptidase 1. Mol Immunol. 2015;67(2 Pt B):426–35. [PubMed: 26224046]
36. Mpakali A, Giastas P, Mathioudakis N, Mavridis IM, Saridakis E, Stratikos E. Structural Basis for Antigenic Peptide Recognition and Processing by Endoplasmic Reticulum (ER) Aminopeptidase 2. J Biol Chem. 2015;290(43):26021–32. [PubMed: 26381406]
37. Giastas P, Mpakali A, Papakyriakou A, Lelis A, Kokkala P, Neu M, et al. Mechanism for antigenic peptide selection by endoplasmic reticulum aminopeptidase 1. Proc Natl Acad Sci U S A. 2019.
38. Rotzschke O, Falk K, Stevanovic S, Jung G, Walden P, Rammensee HG. Exact prediction of a natural T cell epitope. Eur J Immunol. 1991;21(11):2891–4. [PubMed: 1718764]
39. Haeckel R, Hess B, Lauterborn W, Wuster KH. Purification and allosteric properties of yeast pyruvate kinase. Hoppe Seylers Z Physiol Chem. 1968;349(5):699–714. [PubMed: 4386962]
40. Hathaway JA, Atkinson DE. The Effect of Adenylic Acid on Yeast Nicotinamide Adenine Dinucleotide Isocitrate Dehydrogenase, a Possible Metabolic Control Mechanism. J Biol Chem. 1963;238:2875–81. [PubMed: 14063317]
41. Okazaki R, Kornberg A. Deoxythymidine Kinase of Escherichia Coli. I. Purification and Some Properties of the Enzyme. J Biol Chem. 1964;239:269–74. [PubMed: 14114853]
42. Reeves E, Colebatch-Bourn A, Elliott T, Edwards CJ, James E. Functionally distinct ERAP1 allotype combinations distinguish individuals with Ankylosing Spondylitis. Proc Natl Acad Sci U S A. 2014;111(49):17594–9. [PubMed: 25422414]
43. Hutchinson JP, Temponeras I, Kuiper J, Cortes A, Korczynska J, Kitchen S, et al. Common allotypes of ER aminopeptidase 1 have substrate-dependent and highly variable enzymatic properties. J Biol Chem. 2021;296:100443. [PubMed: 33617882]
44. Kochan G, Krojer T, Harvey D, Fischer R, Chen L, Vollmar M, et al. Crystal structures of the endoplasmic reticulum aminopeptidase-1 (ERAP1) reveal the molecular basis for N-terminal peptide trimming. Proc Natl Acad Sci U S A. 2011;108(19):7745–50. [PubMed: 21508329]
45. Maben Z, Arya R, Georgiadis D, Stratikos E, Stern LJ. Conformational dynamics linked to domain closure and substrate binding explain the ERAP1 allosteric regulation mechanism. Nat Commun. 2021;12(1):5302. [PubMed: 34489420]
46. Stamogiannos A, Maben Z, Papakyriakou A, Mpakali A, Kokkala P, Georgiadis D, et al. Critical Role of Interdomain Interactions in the Conformational Change and Catalytic Mechanism

of Endoplasmic Reticulum Aminopeptidase 1. Biochemistry. 2017;56(10):1546–58. [PubMed: 28218509]

47. Rotzschke O, Falk K, Stevanovic S, Gnau V, Jung G, Rammensee HG. Dominant aromatic/aliphatic C-terminal anchor in HLA-B*2702 and B*2705 peptide motifs. Immunogenetics. 1994;39(1):74–7. [PubMed: 8225441]
48. Giastas P, Neu M, Rowland P, Stratikos E. High-Resolution Crystal Structure of Endoplasmic Reticulum Aminopeptidase 1 with Bound Phosphinic Transition-State Analogue Inhibitor. ACS Med Chem Lett. 2019;10(5):708–13. [PubMed: 31097987]
49. Liddle J, Hutchinson JP, Kitchen S, Rowland P, Neu M, Cecconie T, et al. Targeting the Regulatory Site of ER Aminopeptidase 1 Leads to the Discovery of a Natural Product Modulator of Antigen Presentation. J Med Chem. 2020;63(6):3348–58. [PubMed: 32109056]
50. Maben Z, Arya R, Rane D, An WF, Metkar S, Hickey M, et al. Discovery of Selective Inhibitors of Endoplasmic Reticulum Aminopeptidase 1. J Med Chem. 2020;63(1):103–21. [PubMed: 31841350]
51. Reeves E, Islam Y, James E. ERAP1: a potential therapeutic target for a myriad of diseases. Expert opinion on therapeutic targets. 2020;24(6):535–44. [PubMed: 32249641]
52. D'Amico S, Tempora P, Melaiu O, Lucarini V, Cifaldi L, Locatelli F, et al. Targeting the antigen processing and presentation pathway to overcome resistance to immune checkpoint therapy. Front Immunol. 2022;13:948297. [PubMed: 35936007]
53. Sui L, Gandhi A, Guo H-C. Single-Chain Expression and Crystallization of an Antigenic C-Terminus in Complex with the Regulatory Domain of ER Aminopeptidase 1. Crystal Structure Theory and Applications. 2015;4:47–52.
54. Sui L, Guo H-C. Enhanced recombinant expression and purification of human IRAP for biochemical and crystallography studies. Biochem Biophys Rep. 2021;27:101042. [PubMed: 34169156]

(a)

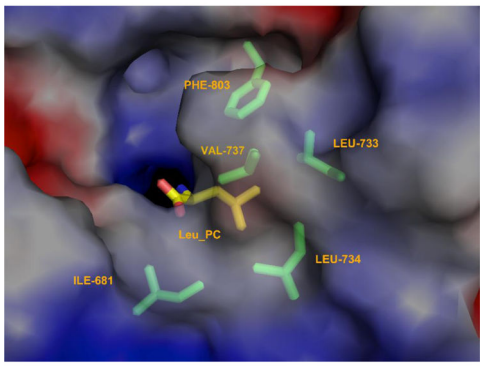

(b)

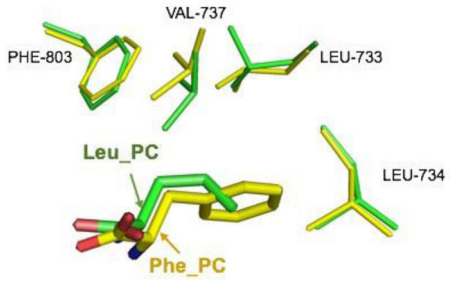

Figure 1. Interactions between substrate PC anchor side chain and the putative ERAP1 specificity subsite SC.

(a) The C-terminus binding cleft of ERAP1 is shown as solvent accessible surfaces colored by electrostatic potentials: from red to blue for negatively charged to positively charged areas. The peptide Leu anchor at the PC position (Leu_PC) is shown as a stick model colored by atom types: yellow for carbons, blue for nitrogen, and red for oxygens. ERAP1 residues surrounding the Leu_PC side chain are shown as turquoise stick models.

(b) Structural superposition of two different peptide PC anchors, Phe_PC and Leu_PC, bound at the same SC hydrophobic pocket around ERAP1 side chains Leu733, Leu734, Val737, and Phe803. Ile681 is omitted here for clarity. Bound peptides in complex with ERAP1 are indicated as thick stick models, whereas side chains forming the ERAP1 specificity pocket are shown as skinny stick models. Atoms of PC anchors and surrounding ERAP1 residues are colored by atom type: yellow for carbons in complex with Phe_PC anchor, green for carbons in complex with Leu_PC anchor, blue for nitrogens, and red for oxygens. Figures are adapted from previous structural reports (32, 33).

(a)

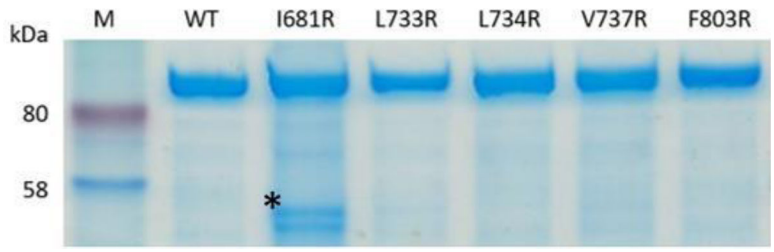

(b)

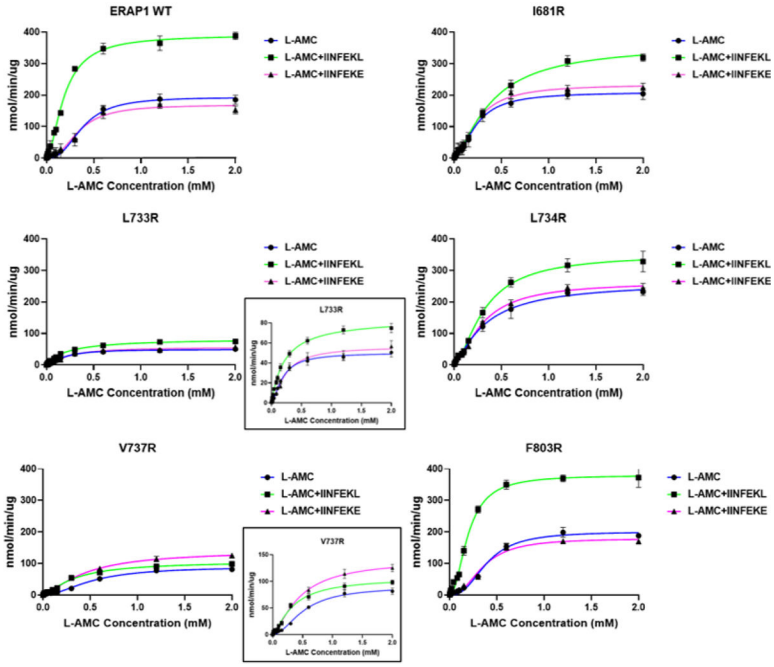

(c)

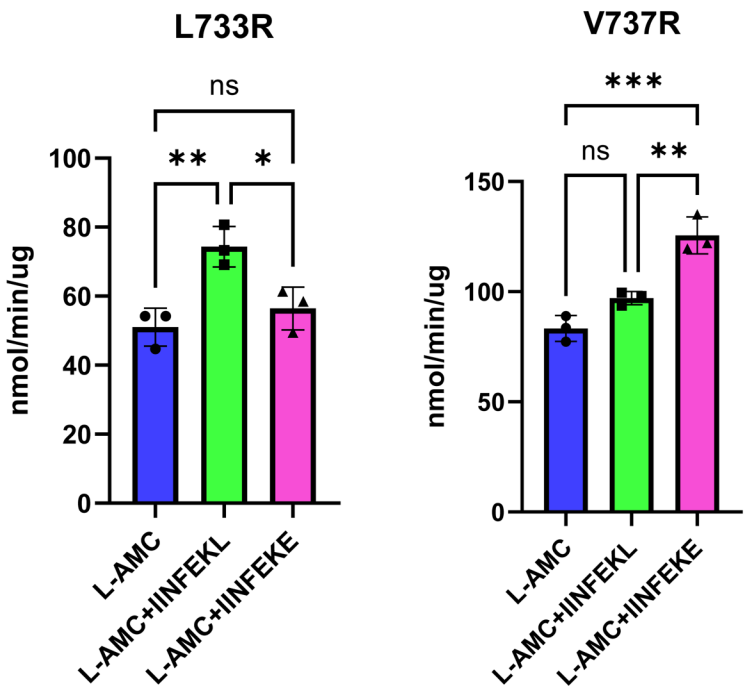

Figure 2. Enzyme variants purification and kinetic analysis of L-AMC hydrolysis in the absence or the presence of IINFEKL or IINFEKE peptide.

(a) SDS-PAGE analysis of purified ERAP1 WT or mutant enzyme, stained with Coomassie blue. Lane M represents molecular weight markers. Note that for I681R mutant, apart from the full length ERAP1 band (~100 kDa), there are two additional bands around 55 kDa (highlighted by *).

(b) Steady state kinetics studies of L-AMC hydrolysis were measured in the absence or the presence of a peptide activator (IINFEKL or IINFEKE) with varying concentrations (0–2,000 μM) of L-AMC. Initial rates (V) were calculated based on reactions at three different time points, and are expressed in unit of nmoles.min^{-1}.μg^{-1} enzyme. In the absence of peptides, L-AMC hydrolysis show positive cooperativity and fits a sigmoidal allosteric curve for all enzymes (blue curves). In the presence of IINFEKL peptide, all variants had an increased activity and followed hyperbolic (Michaelis-Menten) kinetics without apparent cooperativity (green curves). On the other hand, presence of IINFEKE peptide did not significantly change the sigmoidal curve of the enzymes except for the V737R mutant that had a small but significant increase in activity (magenta curves). The insets are zoom-in graphs of L733R and V737R mutants. The assays were performed with 1.5 μg ml^{-1} ERAP1 (WT or mutants) with varying concentrations (0–2,000 μM) of L-AMC at 27 °C, and if applicable with 100 μM of peptide (IINFEKL or IINFEKE). Hydrolysis of L-AMC was followed for 5 minutes. Error bars represent standard errors of three independent repeats (only visible when sufficiently large on the graph).

(c) One-way ANOVA analysis for comparing activities of L733R and V737R in the absence or the presence of a peptide activator (IINFEKL or IINFEKE). Statistics were performed by Brown-Forsyth one-way ANOVA and Tukey's multiple comparisons test, based on the

kinetics data points at the L-AMC concentration of 2.0 mM in (*b*). For L733R, *P* values are *=0.0224, **=0.0067. For V737R, *P* values are **=0.0027, ***=0.0003.

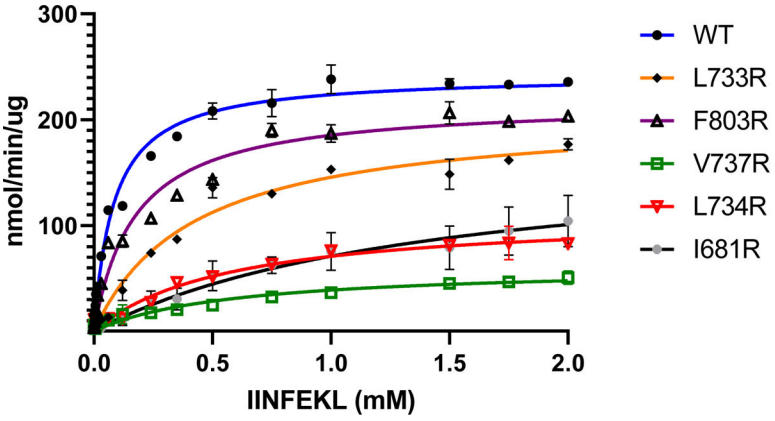

Figure 3. Determination of kinetic parameter AC_{50} for the peptide effector IINFEKL.

Initial rates of L-AMC hydrolysis as a function of peptide concentration are shown for ERAP1 WT, and variants I681R, L733R, L734R, V737R and F803R, and are expressed in unit of nmoles.min^{-1}.μg^{-1} enzyme. Solid lines show the best fit to an equation describing simple Michaelis-Menten kinetics with estimated Vmax and AC50 values listed in Table 2. The assays were performed with 1.5 μg ml^{-1} ERAP1 (WT or mutants) with varying concentrations (0–2,000 μM) of peptide IINFEKL at 27 °C, and with 100 μM of L-AMC. Hydrolysis of L-AMC was followed for 5 minutes. Error bars represent the standard errors of three independent repeats (only visible when sufficiently large on the graph).

(a)

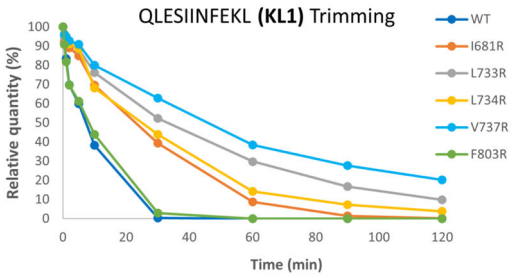

(b)

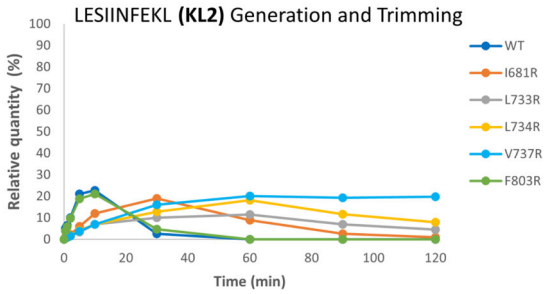

Figure 4. The N-terminal peptide trimming of a natural antigen precursor by ERAP1 variants.

Peptide trimming of ERAP1 WT and mutants were monitored by LC-MS/MS for: (a) the decrease of the initial 11-mer antigen precursor KL1 (QLESIINFEKL), and (b) the concurrent generation and further trimming of the 10-mer product KL2 (LESIINFEKL). Error bars represent the standard errors of two independent experiments (only visible when sufficiently large on the graph). Each data point (relative quantity) was normalized to the starting 11-mer substrate KL1 (at 0-min in (*a*)).

(a)

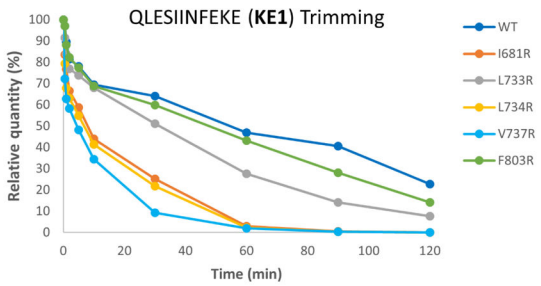

(b)

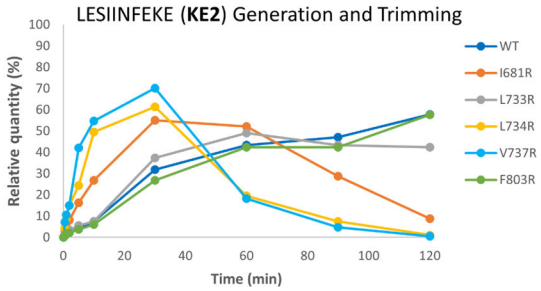

Figure 5. The N-terminal peptide trimming of an altered antigen precursor carrying Glu at the PC position.

Peptide trimming activity on a modified peptide precursor with a negatively charged residue (glutamic acid, E) at the PC position was monitored by LC-MS/MS for: (a) the decrease of the initial 11-mer antigen precursor KE1 (QLESIINFEKE), and (b) the concurrent generation and further trimming of the 10-mer product KE2 (LESIINFEKE). Error bars represent the standard errors of two independent experiments (only visible when sufficiently large on the graph). Each data point (relative quantity) was normalized to the starting 11-mer substrate KE1 (at 0-min in (*a*)).

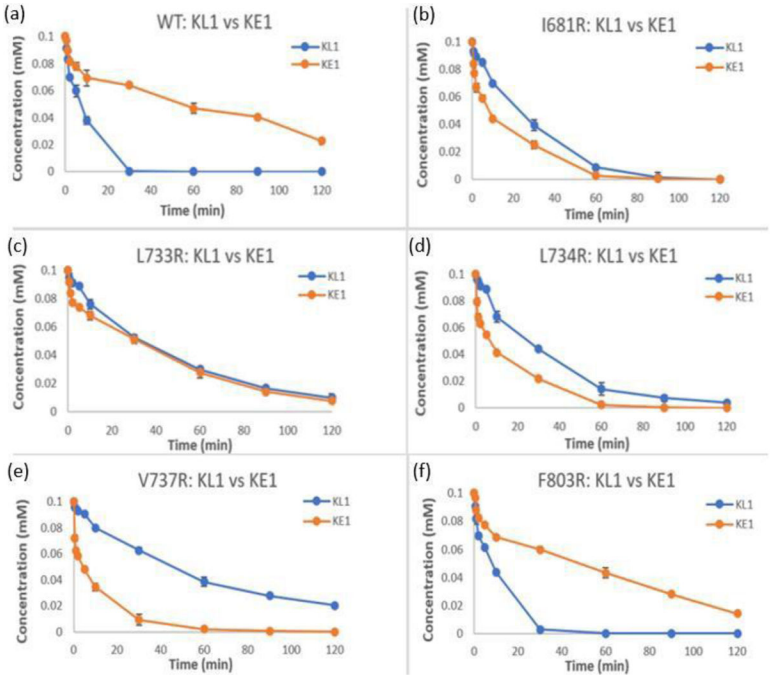

Figure 6. Comparative analyses of N-terminal trimming efficiency on precursor peptides that differ in only the PC anchor: a hydrophobic Leu vs a negatively charged Glu.

LC-MS/MS was used to compare N-terminal trimming efficiency on precursor peptides KL1 (QLESIINFEKL, blue curves) vs KE1 (QLESIINFEKE, orange curves), carrying either a hydrophobic Leu or a negatively charged Glu at the PC position. Comparative analyses are presented for the ERAP1 WT (a), and mutants I681R (b), L733R (c), L734R (d), V737R (e), and F803R (f). Error bars represent the standard errors of two independent experiments (only visible when sufficiently large on the graph).

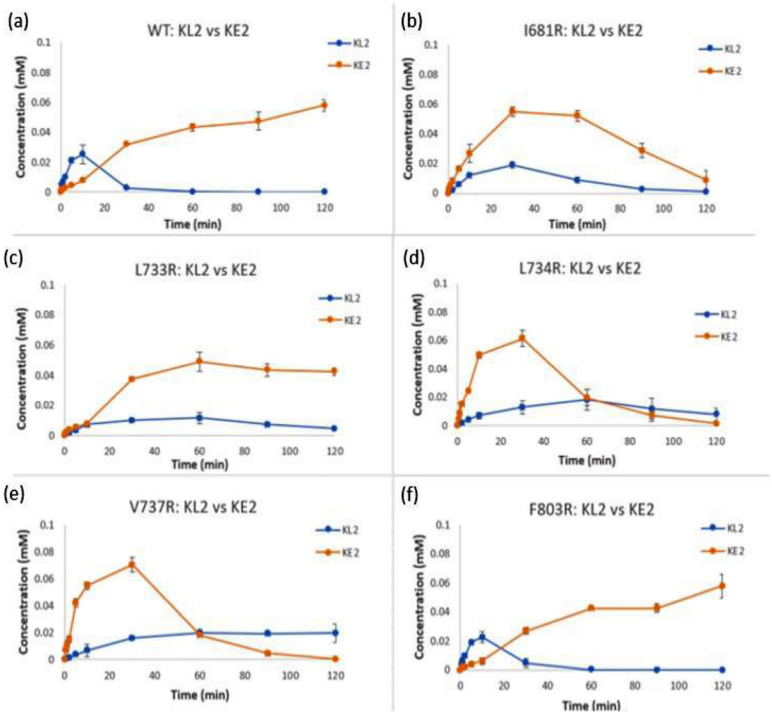

Figure 7. Comparative analyses of concurrent generation and cleavage of the 10-mer peptide intermediate that differ in only the PC anchor: a hydrophobic Leu vs a negatively charged Glu.

LC-MS/MS was used to compare the rate of generation and subsequent cleavage on the peptide intermediates KL2 (LESIINFEKL, blue curves) vs KE2 (LESIINFEKE, orange curves), carrying either a hydrophobic Leu or a negatively charged Glu at the PC position. Comparative analyses are presented for the ERAP1 WT (a), and mutants I681R (b), L733R (c), L734R (d), V737R (e), and F803R (f). Error bars represent the standard errors of two independent experiments (only visible when sufficiently large on the graph).

Table 1.

Kinetic parameters of L-AMC hydrolysis in the absence or the presence of a peptide activator[a].

ERAP1 ± Activator	Vmax (nmol/min/μg)	$K_{1/2}$ (mM)	Hill coef. (h)
Wildtype			
▬	193 ± 8	0.38 ± 0.05	2.6
IINFEKL	391 ± 6	0.19 ± 0.03	2.6
IINFEKE	169 ± 6	0.34 ± 0.08	2.4
I681R			
▬	210 ± 8	0.23 ± 0.04	1.8
IINFEKL	359 ± 5	0.40 ± 0.09	1.4
IINFEKE	234 ± 7	0.24 ± 0.06	1.7
L733R			
▬	50 ± 1	0.19 ± 0.03	1.5
IINFEKL	84 ± 1	0.22 ± 0.04	1.0
IINFEKE	56 ± 1	0.23 ± 0.08	1.4
L734R			
▬	263 ± 4	0.33 ± 0.09	1.3
IINFEKL	351 ± 5	0.33 ± 0.09	1.6
IINFEKE	264 ± 2	0.30 ± 0.07	1.5
V737R			
▬	90 ± 1	0.52 ± 0.09	1.9
IINFEKL	107 ± 1	0.34 ± 0.14	1.4
IINFEKE	141 ± 1	0.34 ± 0.14	1.4
F803R			
▬	200 ± 2	0.39 ± 0.06	2.6
IINFEKL	379 ± 4	0.20 ± 0.03	2.0
IINFEKE	179 ± 1	0.35 ± 0.08	2.3

[a]Kinetic parameters were calculated using the data presented in Figure 2b.

Table 2.

Kinetic parameters of peptide activator IINFEKL for L-AMC hydrolysis[a].

ERAP1	Vmax (nmol/min/μg)	AC_{50} (mM)
Wildtype	241 ± 6	0.08 ± 0.01
I681R	175 ± 54	1.46 ± 0.84
L733R	211 ± 10	0.44 ± 0.06
L734R	112 ± 8	0.58 ± 0.12
V737R	62 ± 7	0.59 ± 0.17
F803R	217 ± 9	0.17 ± 0.03

[a]Kinetic parameters were calculated using the data presented in Figure 3.